# Integrated Modeling and Optimal Operation of Multi-Energy System for Coastal Community

Yang Chen, Jun Chen, *Senior Member, IEEE*, Chenang Liu, Guodong Liu,
Maximiliano Ferrari and Aditya Sundararajan

***Abstract*—Focusing on remote, isolated, and underserved communities, a multi-energy system is designed in this research which is capable of utilizing different energy sources in a more coordinated and energy-efficient way to support various demands, such as fresh water, electricity, hydrogen, thermal demand, etc. The energy sources considered are renewables (wind, solar, marine) and natural gas. The energy conversion process includes water desalination, gas combustion, water electrolyzation, and different types of storage (hydrogen tank, electricity, thermal, etc.) are designed to serve as buffers in supply-demand balancing. Sets of experiments are designed to demonstrate the effectiveness of the proposed operating model and investigate the impact of uncertainties from renewable generations and demands.**

***Index Terms*—Coastal Ccommunity, Multi-Energy Systems, Hydrogen Economy, Water Desalination.**

## I. Introduction

Energy, water, food are integral pillars of coastal infrastructure and essential for human well-being. However, being the frontier of climate challenges, water and sanitation systems of coastal communities are at increased risk to groundwater infiltration and salinization imposed by climate changes. Meanwhile, remote and islandic communities face high energy cost and energy disruptions, for example, Department of Energy announced in April 2021 to support 11 selected island communities (including coastal communities) planning its best way to meet energy needs in a more affordable, resilient, and sustainable way [1]. Compared to onshore solar and wind generation, marine renewables like wave and tidal energy are generally reliable and continuous, easy to predict, and have a variety of ways to be harnessed. The theoretical annual energy potential of waves off the coasts of the United States is estimated to be as much as 2.64 trillion kilowatthours, or the equivalent of about 66% of U.S. electricity generation in 2020 [2]. In April 2021, the National Hydropower Association unveiled its new bold and achievable industry deployment targets of 50 MW by 2025, 500 MW by 2030, and 1 GW by 2035 [3]. Despite of the tremendous potentials, marine renewables suffer from high cost at current stage. Tidal energy is limited by the availability of sites for construction, and wave energy is highly dependent on wave speed and wavelength. These drawbacks have made marine energy not a viable energy source for long-distance inland consumption, and only coastal towns and cities near the ocean can benefit directly from it.

In addition, for the transportation in coastal regions, new emissions regulations by the International Maritime Organization limit the sulfur content in fuel oil used on ships (or "bunker fuel") from 3.5% to 0.5%, starting in 2020. These limits are further reduced to 0.1% for ships operating in Emissions Control Areas, including certain coastal regions of the United States and the European Union. Given such increasingly stringent requirements, hydrogen and hydrogen carriers may offer an attractive alternative to bunker fuel. Furthermore, the use of hydrogen in various marine vessels and at ports for drayage trucks, shore power (electricity for ships while docked), and cargo equipment offers the potential to reduce both carbon dioxide and other emissions and to develop infrastructure in targeted regions [4].

Extensive research has been conducted on different aspects of off-shore renewables, freshwater and hydrogen production. Wave energy resource assessments for US coastal waters have been reported at different scales [5], for instance, regional coastline (West Coast [6], Hawaii [7], East Coast [8] [9], etc.) and national US Coast [10]. Energy hub of heating-cooling-electricity-freshwater is designed for coastal urban by taking economic and emission factors into account [11]. Day-ahead optimal operation of coastal energy hub is modeled as multi-objective problem with energy storage systems (thermal storage, compressed air energy storage) and seawater desalination as flexible load [12]. In [13], a solar-based integrated energy system is designed to provide cooling and hydrogen production via proton exchange membrane electrolysis, and comprehensive parametric study is carried out to understand the effect of major design parameters on system energy, exergy and exergoeconomic. Hydrogen fueling stations are essential to the success of fuel cell electric vehicles. To justify the economic viability, optimal scheduling of privately owned hydrogen storage stations is investigated to serve both transport sector and electricity market operator [14]. As clean and renewable energy, hydrogen is an emerging way to replace fossil fuels. To build a hydrogen-based distributed energy system for the demand side, the optimal planning of such a system is studied with the objective of minimizing annual capital and

Y. Chen is with Department of Industrial and Systems Engineering, North Carolina Agricultural and Technical State University, Greensboro, USA (email: ychen1@ncat.edu)

J. Chen is with Department of Electrical and Computer Engineering, Oakland University, Rochester, MI 48309, USA (email: junchen@oakland.edu)

C. Liu is with School of Industrial Engineeering & Management, Oklahoma State University, Stillwater, USA (email: chenang.liu@okstate.edu)

G. Liu, M. Ferrari and A. Sundararajan are with Electrification and Energy Infrastructures Division, Oak Ridge National Laboratory, Oak Ridge, TN 37831, USA (email: liug@ornl.gov, ferrarimagmf@ornl.gov and sundararajaa@ornl.gov)

Corresponding Author: J. Chen (email: junchen@oakland.edu)

2023 IEEE International Conference on Electro Information Technology (eIT) | 978-1-6654-9376-5/23/$31.00 ©2023 IEEE | DOI: 10.1109/EIT57321.2023.10187307

operation expenditure [15]. Hydrogen storage units, hot water, and chilled water storage units are coordinated together to improve energy efficiency and reduce system costs.

Motivated by the thermal, fresh water, and potential hydrogen demand on coastal communities, we propose to design a comprehensive multi-energy system aiming to improve energy utilization efficiency and support the coastal blue economy. In Section II, the systematic configuration of the proposed multi-energy system is presented along with the basic component modeling; in Section III, different sets of case studies are designed to demonstrate the effectiveness of the proposed model. Finally, conclusions are drawn in Section IV.

## II. Multi-Energy System Scheme and Modeling

The schematic of proposed multi-energy system is shown in Figure 1. The system components can be further categorized as different phases: Resource, Conversion Process, Storage, and Demand.

*Resources:* On the generation side, the resources include seawater resources as feedstock to desalination plant to be purified into potable water, natural gas as input to gas boiler to be converted into electricity and renewable resources (wind, PV solar, wave energy) to be harvested by appropriate devices and converted into electricity.

*Conversion process:* During this process, water desalination plant consumes seawater, electricity or potentially thermal energy depends on desalination technologies, to produce potable water; gas boiler and turbine consumes natural gas to generate electricity through combustion, boiler, and power cycle; and electrolyzer consumes seawater and electricity to produce hydrogen.

*Industrial scale storage:* To better balance supply and demand of each product, the corresponding storage is integrated as buffer. For example, water tank temporally stores the fresh water produced by desalination plant; thermal storage temporally stores the thermal energy produced by the gas turbine; hydrogen tank temporally stores the hydrogen produced by electrolyzer; and battery temporally stores the electricity.

*Demands:* Residential water demand, thermal demand, electricity demand and hydrogen demand from the transportation sector are considered on the demand side.

In the following subsections, operation constraints are presented and explained for each system component.

### A. Renewables

The generated power of wind turbine is modeled as a static mapping function of wind speed [16]–[19], as follows:

$$pW_t = \begin{cases} 0.5 \cdot \eta_w \cdot \rho_{air} \cdot V_t^3 \cdot \frac{\pi \cdot d^2}{4} & \text{if } 3 < V_t \leq 14 \\ 1.5 & \text{if } 14 < V_t < 25 \\ 0 & \text{else} \end{cases}, \tag{1}$$

where $\eta_w$ is the conversion efficiency of the wind turbine, $\rho_{air}$ is the density of the air at the site, $V_t$ (m/s) is the wind speed, and $d$ is the diameter of the turbine blades. For a turbine with rated power of 1.5 MW, the values used for each parameter in equation (1) are: $\eta = 35\%$, $\rho$= 1.17682 (g/m$^3$), $d$ = 58.13 (m). For this study, the wind speed data is downloaded from Eastern Wind Dataset maintained by National Renewable National Laboratory*.

The generated power of PV modeled as a static mapping function of global horizontal irradiance [20], as follows:

$$pS_t = \Omega_t \cdot \tau_{pv} \cdot \eta_{ref} \cdot A \cdot [1 - \gamma \cdot (T_t - 25)], \tag{2}$$

where $T_t$ is the ambient temperature in Celsius, and $A$ is the total area (m$^2$) of the PV module receiving solar irradiation $\Omega_t$ (kWh/m$^2$). The values of parameters in Eqs. (2) used in simulation are: $\tau_{pv} = 90\%$, $\eta_{ref} = 15\%$, and $\gamma = 0.45\%$. For this study, the solar irradiation data is downloaded from National Solar Radiation Database maintained by National Renewable National Laboratory†.

The generated power $pV_t$ of wave energy harvest device is modeled by the Wave Energy Converter SIMulator (WEC-Sim) developed by National Renewable National Laboratory‡.

Therefore, the total renewable power output, in terms of electricity, is denoted as

$$pR_t = pW_t + pS_t + pV_t. \tag{3}$$

### B. Desalination

The reverse osmosis desalination plant consumes electricity and push the seawater through a reverse osmosis membrane to produce fresh water. The total power consumption $pD_t$ by desalination plants is calculated as a production of water flow rate $wf_t$ and desalination specific energy consumption $ds_t$ (kWh/m$^3$) in Eq.(4), as follows.

$$pD_t \cdot 1000 = ds_t \cdot wf_t \tag{4}$$

$$ds_t = 2.05 \cdot 10^{-5} \cdot C_0 \cdot \frac{2 - R}{2 \cdot (1 - R)} + 2.78 \cdot 10^{-7} \cdot R_m \cdot wf_t, \tag{5}$$

where $ds_t$ itself is a function of $wf_t$ in Eq.(5). $R$ is the water recovery ratio of the process and $R_m$ is the membrane resistance, $C_0$ is initial salt concentration of feed water. Eq.(4) and Eq.(5) are adopted from reference [21]. Values $C_0$ = 36000 (ppm), $R$ = 0.55, $R_m$ = 33.95 (Pa.Sec/m) are used here.

### C. Combined Heat and Power (CHP)

In CHP, the gas turbine can generate both electric power and heat while gas boiler is the heat generator. Here, $pT_t$ is power generated by gas turbine, $qT_t$ is the thermal generated by gas turbine, $qB_t$ is the thermal generated by gas boiler, $gT_t$ is the gas input for gas turbine, $gB_t$ is the gas input for gas boiler. $Vg$ low calorific value of gas. $\eta_T$ is the generation efficiency of gas turbine, $\eta_Q$ is the thermal generation efficiency of gas boiler. $\eta_L$ is the heat loss coefficient of gas turbine, $\eta_X$ is the

*The data is accessible at https://www.nrel.gov/grid/eastern-wind-data.html

†The data is accessible at https://nsrdb.nrel.gov/

‡The simulator is accessible at https://wec-sim.github.io/WEC-Sim/

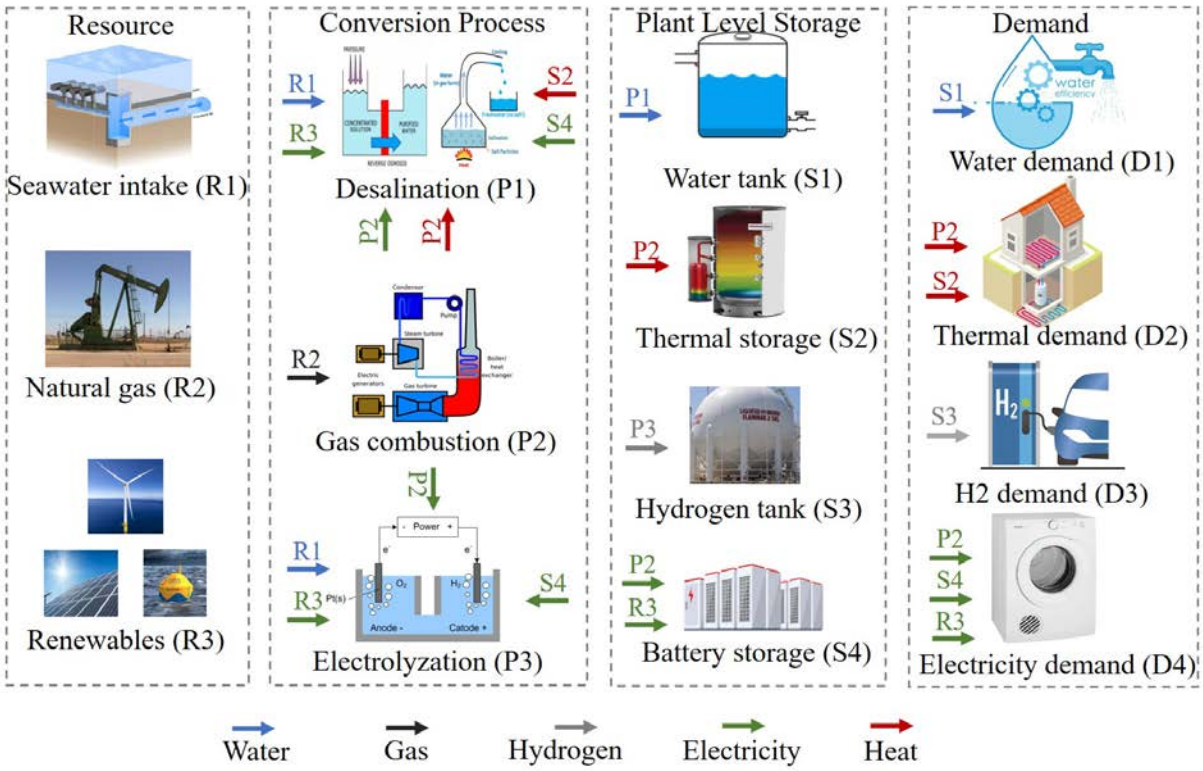


Fig. 1: The scheme of multi-energy system for coastal community

heat exchanger coefficient. Eq.(6)-(8) are modified based on reference [22], as follows.

$$pT_t = gT_t \cdot Vg \cdot \eta_T \tag{6}$$

$$qT_t \leq \eta_X \cdot pT_t \cdot (1 - \eta_T - \eta_L)/\eta_T \tag{7}$$

$$qB_t \leq gB_t \cdot Vg \cdot \eta_Q \tag{8}$$

Values $\eta_T$ = 0.35, $\eta_Q$ = 0.65, $\eta_L$ = 0.5, $\eta_X$ = 0.5, $Vg$ = 0.0097 (MWh/m$^3$) are used here.

### D. Electrolyzer

Hydrogen production is calculated based on Eq.(9) [23],

$$hf_t = \eta_Z \cdot pZ_t \cdot PH, \tag{9}$$

where $hf_t$ is the hydrogen production flow, $\eta_Z$ is the efficiency of electrolyzer, $pZ_t$ is power input for electrolyzer, $PH$ is the power to hydrogen conversion factor. Values $PH$ = 360 (m$^3$/MWh) and $\eta_Z$ = 0.6 are used here.

### E. Storage or Tank

For storages or tanks, the general dynamic of charging/discharging activities can be modeled in Eqs. (10)-(13) [24] [25], as follows.

$$px_t = px_t^+ - px_t^- \tag{10}$$

$$s_t = s_{t-1} - \frac{px_t^-}{\eta_D} + px_t^+ \cdot \eta_C \tag{11}$$

$$-Cs \cdot \alpha \leq px_t \leq Cs \cdot \alpha \tag{12}$$

$$0 \leq s_t \leq Cs, \tag{13}$$

where $px_t^+$ and $px_t^-$ are charging and discharging amount, $px_t$ is the resulted charging or discharging amount (could be positive or negative), $s_t$ is the storage level, $Cs$ is the storages or tanks capacity. $\eta_C$ and $\eta_D$ denote the discharge and charge efficiency of the storages or tanks. For thermal storage $\eta_C = \eta_D = 0.85$, $Cs$ = 1.5 (MW); for battery $\eta_C = \eta_D = 0.9$, $Cs$ = 1 (MW), for water tank $\eta_C = \eta_D = 1$, $Cs$ = 50 (m$^3$), and for hydrogen tank $\eta_C = \eta_D = 1$, $Cs$ = 200 (m$^3$). For all storages and tanks, $\alpha = 0.25$ is the maximum charging or discharging efficiency.

### F. Demand Balance

From the system scheme shown in Figure 1, the following demand balance equations can be derived. Note that, $px$ represent charging or discharging amount for water, thermal, hydrogen and power in Eq. (14), (15), (16) and (17), respectively.

$$wf_t + px_t = Dw_t \tag{14}$$

$$qT_t + qB_t + px_t = Dq_t \tag{15}$$

$$hf_t + px_t = Dh_t \tag{16}$$

$$pR_t + pT_t + px_t - pD_t - pZ_t = Dp_t \tag{17}$$

The demands are modeled as time series data obtained from various sources. For example, the building thermal demand $Dq_t$ and electricity power demand $Dp_t$ are available from public database [26] or [27]. The hydrogen demand $Dh_t$ is available in reference [23] or can be converted from daily

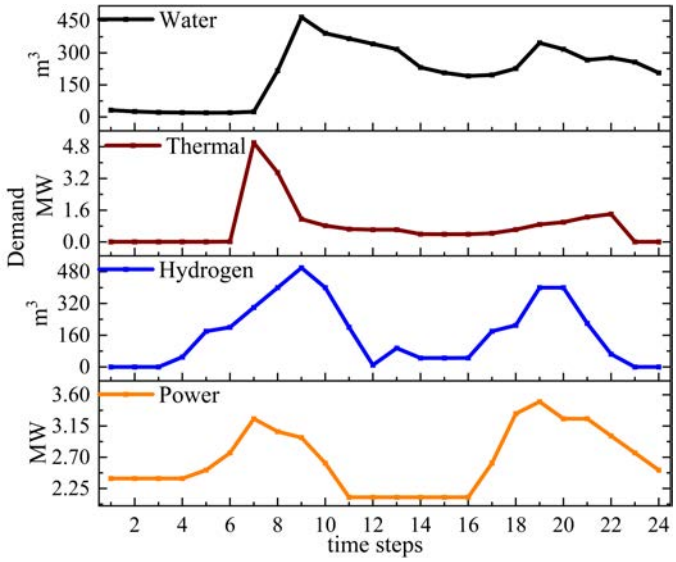


Fig. 2: Multiple demands level in the system.

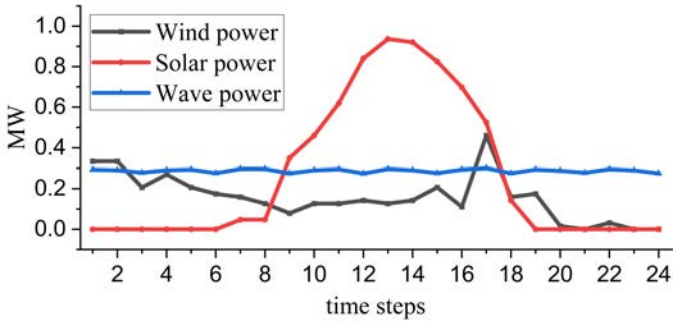


Fig. 3: Renewable generations in the system.

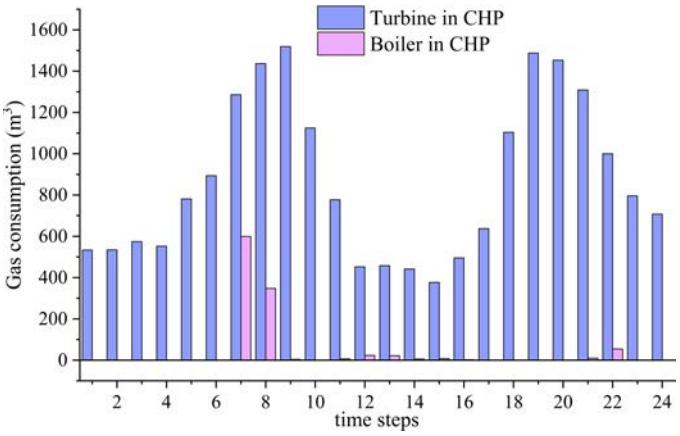


Fig. 4: Gas consumption of CHP.

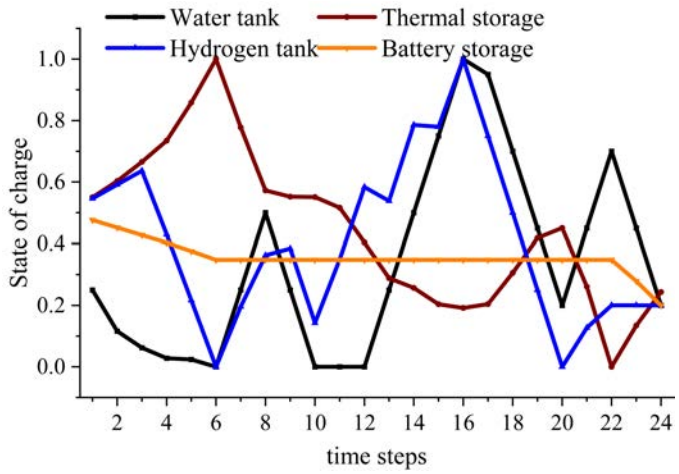


Fig. 5: State of charge for the storages and tanks.

gasoline demand in [28]. The water demand profile $Dw_t$ is available in reference [12].

## III. Numerical Experiments

In this section, the used data and several groups of experiments are presented. The hourly demand level of different products are plotted in Figure 2, and the renewable power generations are shown in Figure 3.

To demonstrate the proposed operation model in Section II, two different operation cases are considered here.

### A. Day-ahead Operation

In this case, the optimization model is solved once with known hourly day-ahead data as input. The complete model can be summarized as in model (18).

$$\min \quad \textstyle\sum_t (gT_t + gB_t) \tag{18a}$$

$$\text{s.t.} \quad Eq.(1) - (17) \tag{18b}$$

The optimization objective is to minimize total gas consumption here. Assume the demand and generation are known day-ahead, the minimum gas consumption is 21814.83 ($m^3$) based on current parameter settings. Figure 4 shows the hourly gas consumption of CHP. The state of charge for storages and tanks is shown in Figure 5. Note that, the state of charge at the beginning of the day are initialized as 50% and are required to be greater than 20% at the end of the day. Since thermal energy can only be provided from CHP and thermal storage, it can be observed from Figure 4 that, gas consumption is concentrated around hour 7 and 8 to satisfy thermal demand peak, and thermal storage is charged to full in Figure 5 before the peak hour 7 for subsequent discharging.

### B. Rolling-Horizon Operation

To make more practical decisions with the uncertainties from renewables and demands, stochastic rolling-horizon operation is also considered here by Model Predictive Control (MPC) approach. Suppose current time step is $t-1$, depends on the demand prediction time window $w$, the main solving procedure using MPC approach is as follows:

i Predict renewables and demands for a future horizon window $t+w$ before the current time step $t$.

ii Solve the model (18) for time dimension $t+w$ to obtain charging or discharging amount decisions.

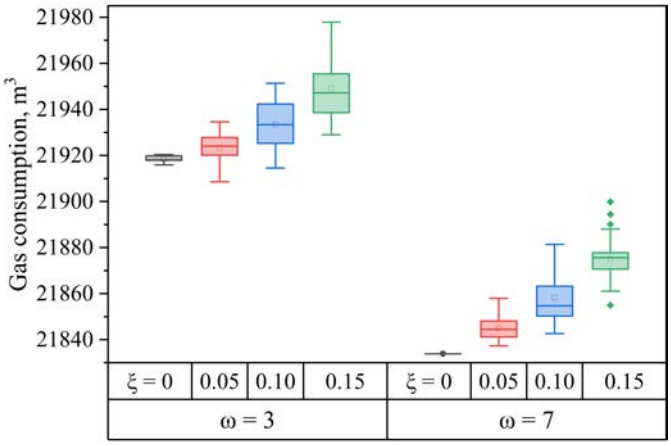


Fig. 6: Gas consumption in rolling-horizon operation considering the uncertainties.

iii Fix the charging or discharging decisions in time step $t$ and solve the model (18) only in time step $t$ when the demands become certain.

iv Obtain state of charge level of storages and tanks in time step $t$ which are inputs for next iteration in $t+1$.

v Repeat the previous steps until last time step.

For the sake of simplicity, we assume the look-ahead window $t+w=4$ ($w$ = 3) and $t+w=8$ ($w$ = 7) hours and the prediction error $\xi$ is within different ranges: $\pm$ 0%, $\pm$ 5%, $\pm$ 10% and $\pm$ 15% based on the true demands in Figure 2 and Figure 3 for each time step.

With the data sampling, for each parameter setting, the experiment is run 30 times to get the objectives. The objective distribution is shown in Figure 6. For instance, when look-ahead window $w$ = 3 and error range $\xi = 0.15$, the 30 objective points locate in range [21928, 21977], and similarly, the range is [21854, 21899] for $w$ = 7 and $\xi$ = 0.15. It indicates that it's better to have more information on the renewables and demands in near future even though with 15% prediction error. It also shows that the worst objective with $w$ = 7 and $\xi$ = 0.15 is still better than the objective $w$ = 3 and prediction error $\xi$ = 0 (accurate prediction). The similar trend can be observed for different prediction error $\xi$. Note that, the objective (21833) with $w$ = 7 and $\xi$ = 0 is slightly worse than the optimal objective (21814) in day-ahead operation. The results in this section could also imply the bound of the information value if purchasing more accurate prediction services.

## IV. Conclusion

In this work, social welfare for the coastal community is focused. Specifically, we have proposed a comprehensive multi-energy system to satisfy the needs of freshwater, hydrogen, and thermal production in an integrated way. Based on the system framework, an operating model is established to coordinate the multiple conversion processes and storage operations. The effectiveness of the proposed model is demonstrated by day-ahead operation. The impact of uncertainties on the objective is illustrated by parametric studies of the look-ahead time windows and prediction errors in the model predictive control approach. In the future, more interactions between the proposed multi-energy system and energy markets will be investigated, together with Monte Carlo simulation using synthetic dataset [29] and detailed battery modeling [30]–[32].

## References

[1] Department of Energy, "DOE to support 11 remote and island communities transitioning to resilient clean energy soltuions." [Online]. Available: https://www.energy.gov/articles/doe-support-11-remote-and-island-communities-transitioning-resilient-clean-energy

[2] U. E. I. Administration, "Waves have a lot of energy." [Online]. Available: https://www.eia.gov/energyexplained/hydropower/wave-power.php

[3] National Hydropower Association, "Marine Energy Industry Sets New Goal Of 1GW of Deployments by 2035." [Online]. Available: https://www.hydro.org/news/marine-energy-industry-sets-new-goal-of-1gw-of-deployments-by-2035/

[4] U.S. Department of Energy, "Department of Energy Hydrogen Program Plan." [Online]. Available: https://www.hydrogen.energy.gov/pdfs/hydrogen-program-plan-2020.pdf

[5] S. Ahn, K. A. Haas, and V. S. Neary, "Dominant Wave Energy Systems and Conditional Wave Resource Characterization for Coastal Waters of the United States," *Energies*, vol. 13, no. 12, p. 3041.

[6] Z. Yang, G. García-Medina, W.-C. Wu, and T. Wang, "Characteristics and variability of the nearshore wave resource on the U.S. West Coast," *Energy*, vol. 203, p. 117818, Jul. 2020.

[7] J. E. Stopa, K. F. Cheung, and Y.-L. Chen, "Assessment of wave energy resources in Hawaii," *Renewable Energy*, vol. 36, no. 2, pp. 554–567, Feb. 2011.

[8] C. Ozkan and T. Mayo, "The renewable wave energy resource in coastal regions of the Florida peninsula," *Renewable Energy*, vol. 139, pp. 530–537, Aug. 2019.

[9] M. N. Allahdadi, B. Gunawan, J. Lai, R. He, and V. S. Neary, "Development and validation of a regional-scale high-resolution unstructured model for wave energy resource characterization along the US East Coast," *Renewable Energy*, vol. 136, pp. 500–511, Jun. 2019.

[10] M. Lehmann, F. Karimpour, C. A. Goudey, P. T. Jacobson, and M.-R. Alam, "Ocean wave energy in the United States: Current status and future perspectives," *Renewable and Sustainable Energy Reviews*, vol. 74, pp. 1300–1313, Jul. 2017.

[11] M. Mostafavi Sani, H. Mostafavi Sani, M. Fowler, A. Elkamel, A. Noorpoor, and A. Ghasemi, "Optimal energy hub development to supply heating, cooling, electricity and freshwater for a coastal urban area taking into account economic and environmental factors," *Energy*, vol. 238, p. 121743, Jan. 2022.

[12] M. Jalili, M. Sedighizadeh, and A. Sheikhi Fini, "Optimal operation of the coastal energy hub considering seawater desalination and compressed air energy storage system," *Thermal Science and Engineering Progress*, vol. 25, p. 101020, Oct. 2021.

[13] A. Behzadi, A. Habibollahzade, P. Ahmadi, E. Gholamian, and E. Houshfar, "Multi-objective design optimization of a solar based system for electricity, cooling, and hydrogen production," *Energy*, vol. 169, pp. 696–709, Feb. 2019.

[14] N. A. El-Taweel, H. Khani, and H. E. Z. Farag, "Hydrogen Storage Optimal Scheduling for Fuel Supply and Capacity-Based Demand Response Program Under Dynamic Hydrogen Pricing," *IEEE Transactions on Smart Grid*, vol. 10, no. 4, pp. 4531–4542, Jul. 2019.

[15] J. Liu, Z. Xu, J. Wu, K. Liu, and X. Guan, "Optimal planning of distributed hydrogen-based multi-energy systems," *Applied Energy*, vol. 281, p. 116107, Jan. 2021.

[16] J. Chen and H. E. Garcia, "Economic optimization of operations for hybrid energy systems under variable markets," *Applied energy*, vol. 177, pp. 11–24, 2016.

[17] J. S. Kim, J. Chen, and H. E. Garcia, "Modeling, control, and dynamic performance analysis of a reverse osmosis desalination plant integrated within hybrid energy systems," *Energy*, vol. 112, pp. 52–66, 2016.

[18] J. Chen, Z. Li, and X. Yin, "Optimization of energy storage sizing and operation for nuclear-renewable-ev hybrid energy systems," in *2021 IEEE Green Technologies Conference*. IEEE, 2021.

[19] J. Chen, H. E. Garcia, J. S. Kim, and S. M. Bragg-Sitton, "Operations optimization of nuclear hybrid energy systems," *Nuclear Technology*, vol. 195, no. 2, pp. 143–156, 2016.
[20] H. E. Garcia, J. Chen, J. S. Kim, R. B. Vilim, W. R. Binder, S. M. B. Sitton, R. D. Boardman, M. G. McKellar, and C. J. Paredis, "Dynamic performance analysis of two regional nuclear hybrid energy systems," *Energy*, vol. 107, pp. 234–258, 2016.
[21] F. Mohammadi, M. Sahraei-Ardakani, Y. M. Al-Abdullah, and G. T. Heydt, "Coordinated scheduling of power generation and water desalination units," *IEEE Transactions on Power Systems*, vol. 34, no. 5, pp. 3657–3666, 2019.
[22] Z. Liu, Y. Chen, R. Zhuo, and H. Jia, "Energy storage capacity optimization for autonomy microgrid considering chp and ev scheduling," *Applied Energy*, vol. 210, pp. 1113–1125, 2018. [Online]. Available: https://www.sciencedirect.com/science/article/pii/S0306261917308656
[23] N. A. El-Taweel, H. Khani, and H. E. Z. Farag, "Hydrogen storage optimal scheduling for fuel supply and capacity-based demand response program under dynamic hydrogen pricing," *IEEE Transactions on Smart Grid*, vol. 10, no. 4, pp. 4531–4542, 2019.
[24] Y. Chen and M. Hu, "Swarm intelligence–based distributed stochastic model predictive control for transactive operation of networked building clusters," *Energy and Buildings*, vol. 198, pp. 207–215, Sep. 2019.
[25] Y. Chen, B. Park, X. Kou, M. Hu, J. Dong, F. Li, K. Amasyali, and M. Olama, "A comparison study on trading behavior and profit distribution in local energy transaction games," *Applied Energy*, vol. 280, p. 115941, Dec. 2020.
[26] OpenEI, "Commercial and Residential Hourly Load Profiles for all TMY3 Locations in the United States."
[27] Z. Liu, Y. Chen, R. Zhuo, and H. Jia, "Energy storage capacity optimization for autonomy microgrid considering CHP and EV scheduling," *Applied Energy*, vol. 210, pp. 1113–1125, Jan. 2018.
[28] L. Tiax, "H2a hydrogen delivery infrastructure analysis models and conventional pathway options analysis results," *Interim Report*, 2008.
[29] J. Chen and C. Rabiti, "Synthetic wind speed scenarios generation for probabilistic analysis of hybrid energy systems," *Energy*, vol. 120, pp. 507–517, 2017.
[30] J. Chen, A. Behal, and C. Li, "Active cell balancing by model predictive control for real time range extension," in *2021 IEEE Conference on Decision and Control*, Austin, TX, USA, December 13–15, 2021.
[31] J. Chen, Z. Zhou, Z. Zhou, X. Wang, and B. Liaw, "Impact of battery cell imbalance on electric vehicle range," *Green Energy and Intelligent Transportation*, vol. 1, no. 3, pp. 1–8, December 2022.
[32] J. Chen and Z. Zhou, "Battery cell imbalance and electric vehicles range: Correlation and NMPC-based balancing control," in *2023 IEEE International Conference on Electro Information Technology*, Romeoville, IL, May 18–20, 2023.